Spiral site percolation on the square and triangular lattices

1992 J. Phys. A: Math. Gen. 25 1105

(http://iopscience.iop.org/0305-4470/25/5/018)

J. Phys. A: Math. Gen. 25 (1992) 1105–1118. Printed in the UK

Spiral site percolation on the square and triangular lattices

S B Santra and I Bose

Department of Physics, Bose Institute, 93/1 Acharya Prafulla Chandra Road, Calcutta-700009, India

Received 15 August 1991, in final form 17 October 1991

Abstract. Percolation under rotational constraint is studied on the square and triangular lattices by three different methods: finite-size scaling study, Monte Carlo simulation and series expansion. The critical percolation probability p_c and some critical exponents are determined. Evidence is obtained for a scaling form of the cluster distribution function. For the square lattice, the average cluster size exponent γ is found to be equal to that of directed percolation.

1. Introduction

Percolation under rotational constraint, referred to as spiral percolation, has recently been studied (Santra and Bose 1991, paper I) on the square lattice using finite-size scaling analysis. In spiral percolation, each path proceeds either straight or in a specific rotational direction, say clockwise. Percolation occurs if a cluster obeying the rotational constraint spans the underlying lattice. For this model, the critical percolation probability p_c for site percolation on the square lattice and some of the critical exponents have been determined in paper I. Evidence has been obtained for a scaling form of the cluster size distribution function. Spiral percolation has been found to belong to a new universality class different from those corresponding to undirected and directed percolation. In section 2 of this paper, we present the results of a finite-size scaling study of spiral site percolation on the triangular lattice for lattice size up to 130×130. Some of the results for the square lattice, given in paper I, are re-examined. Section 3 gives results of Monte Carlo simulation of spiral site percolation on the square (size 140×140) and triangular (size 130×130) lattices. Section 4 contains results for the average cluster size exponent γ for percolation on the square lattice, obtained by the method of series expansion. Section 5 gives a discussion of the results obtained.

2. Finite-size scaling study

This section contains the formulae and procedural details for calculation of some critical exponents to be defined below. We consider spiral site percolation on a triangular lattice of size $L\times L$. For the triangular lattice, the specific rotational direction in which turning is allowed is chosen to be the clockwise direction which has the least deviation from the original direction of motion. The spiral percolation threshold $p_c(L)$ is determined by the binary search method (paper I). The average value $\langle p_c(L)\rangle$ of N estimates ($N\times L\times L$ is of the order of 10^6–10^7) is taken as the percolation threshold. In the case of undirected percolation, the most widely used method of calculating

0305-4470/92/051105+14$04.50

critical exponents is to fill up a large lattice by clusters of various sizes s with site occupation probability p. The cluster size distribution is given by $n_s(p)$, the number of clusters of size s per site of the lattice. The various moments of $n_s(p)$ given by

$$\sum_s{}' s^k n_s(p) \qquad k=0, 1, 2, \ldots \tag{1}$$

(the prime denotes that the largest cluster is excluded from the sum) become singular as $p \to p_c$ with characteristic critical exponents. For example, the average cluster size corresponds to $k=2$ and diverges as $p \to p_c$ with an exponent γ. Thus, a knowledge of $n_s(p)$ and its various moments is necessary for the calculation of critical exponents. Another method for the calculation of critical exponents is the single cluster growth method (Leath 1976, Alexandrowitz 1980) in which clusters are grown singly starting from a fixed origin. The cluster size distribution is now given by

$$P_s(p) = N_s / N_{\text{tot}} \tag{2}$$

where N_s is the number of clusters of size s in a total number N_{tot} of clusters generated. The various moments of $P_s(p)$, $\sum_s{}' s^k P_s(p)$ become singular as $p \to p_c$. The average cluster size χ is given by

$$\chi \sim \sum_s{}' s P_s(p) \tag{3}$$

and diverges as $p \to p_c$ with the critical exponent γ. In the single cluster growth method the cluster configurations are rooted at the origin and the first, not the second, moment of the cluster size distribution defines the exponent γ. In fact, any exponent which corresponds to the kth moment of the cluster size distribution in the case of the lattice-filling method is obtained from the $(k-1)$th moment, one order less, in the case of the single cluster growth method. In the cases of directed and spiral percolation where there is a directionality constraint on the percolation process, one realizes that the cluster size distribution $n_s(p)$ of the lattice-filling method has no meaning. Percolation clusters obeying a directionality constraint can be defined only with respect to a fixed origin. Thus, the single cluster growth method provides the only known simulation procedure for calculation of critical exponents. As in paper I, we combine the single cluster growth method and finite-size scaling analysis in order to calculate various critical quantities. For a particular lattice size $L \times L$ we choose p to be equal to $\langle p_c(L) \rangle$. The values of $\langle p_c(L) \rangle$ for different values of L are listed in table 1. Ten thousand clusters are grown for this value of p. As in paper I, clusters are counted in bins. The size of the largest cluster which spans the lattice, S_∞, is determined. The average cluster size χ given by (3) and also the second moment of the cluster size distribution χ' ($\chi' \sim |p - p_c|^{-\gamma'}$) are calculated. The procedure is repeated for various values of L. In a finite system, quantities like the average cluster size depend not only on p but also on the linear dimension L of the lattice. True critical behaviour occurs only in the limit of infinitely large lattices but an estimate of the critical exponents, e.g. γ, can be obtained from the studies of finite systems by assuming the finite-size scaling hypothesis (Stauffer 1985), which leads to the formula

$$A = L^{-x/\nu} F[(p - p_c) L^{1/\nu}] \tag{4}$$

where A is a quantity which becomes critical, $A \sim |p - p_c|^x$ as $p \to p_c$. The function F is a suitable scaling function. At $p = p_c$, the quantity A varies as $L^{-x/\nu}$. This result can be used to determine the exponents γ/ν, γ'/ν by calculating the first and second

Table 1. The values of percolation threshold $\langle p_c(L)\rangle$ for different values of L for spiral site percolation on the square and triangular lattices.

	$\langle p_c(L)\rangle$	
L	Square lattice	Triangular lattice
30	0.6997	0.6678
40	0.7020	0.6675
50	0.7039	0.6675
60	0.7053	0.6675
70	0.7067	0.6665
80	0.7074	0.6665
90	0.7083	0.6666
100	0.7083	0.6666
110	0.7093	0.6666
120	0.7093	0.6667
130	0.7101	0.6667
140	0.7107	

moments, χ and χ' respectively, of the cluster size distribution. The largest cluster spanning the lattice is of size S_∞ and is a fractal with fractal dimension D defined by

$$S_\infty \sim L^D. \tag{5}$$

The fractal dimension D can again be written as

$$D = d - \beta/\nu \tag{6}$$

where β is the exponent corresponding to the probability P that a site belongs to the infinite (spanning) cluster, $P \sim (p - p_c)^\beta$. From (5) the fractal dimension D can be determined and from (6), putting $d = 2$, the value of β/ν can be calculated.

Figure 1 shows a plot of the logarithm of the largest spanning cluster size S_∞ at the percolation threshold $p_c = \langle p_c(L)\rangle$ versus log L. The slope of the straight line gives

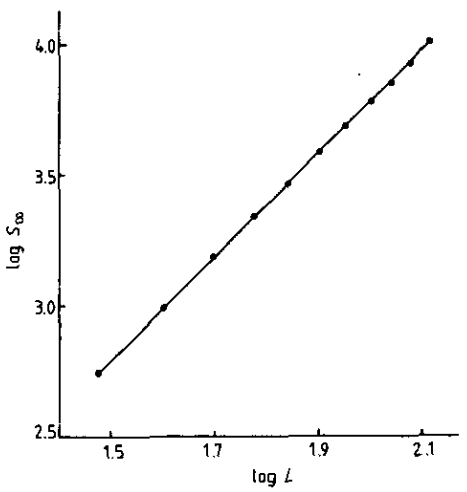

Figure 1. For the triangular lattice, a plot of log S_∞ against log L at $p = \langle p_c(L)\rangle$ where S_∞ is the largest spanning cluster size. The slope of the straight line gives the fractal dimension D of the spanning cluster $D = 1.956 \pm 0.008$.

fractal dimension $D = 1.965 \pm 0.008$ and so from (6) $\beta/\nu = 0.035 \pm 0.008$. In figure 2 the logarithm of the average cluster size χ (equation (3)) is plotted aginst log L at the percolation threshold. The slope of the straight line obtained gives $\gamma/\nu = 1.867 \pm 0.028$. Figure 3 shows a plot of the logarithm of χ', the second moment of the cluster-size distribution, versus log L. The slope of the straight line obtained gives the exponent $\gamma'/\nu = 3.829 \pm 0.062$. The errors quoted for D, γ/ν and γ'/ν are the standard least square fit errors taking into account the statistical error of each single data point. In paper I, spiral site percolation on the square lattice was considered. In that paper, the exponent γ/ν was wrongly calculated from the second moment, rather than the first moment of the cluster size distribution. We have rectified the error by recalculating the exponent γ/ν from the first moment of $P_s(p)$. The correct values of the exponents γ/ν and γ'/ν are $\gamma/\nu = 2.01 \pm 0.06$, $\gamma'/\nu = 4.05 \pm 0.13$. The exponent β/ν as computed in paper I is $\beta/\nu = 0.043 \pm 0.009$. In paper I, the correlation length exponent ν was determined by using the finite-size scaling formula (Levinshtein *et al* 1976, Reynolds

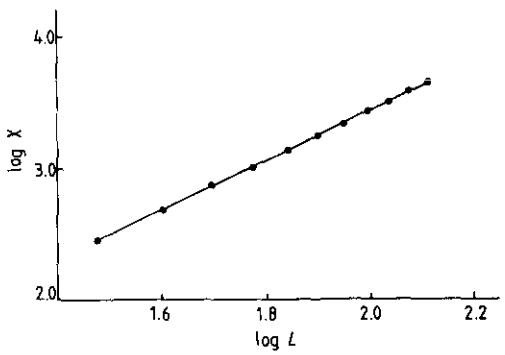

Figure 2. For the triangular lattice, a plot of log χ against log L at $p = \langle p_c(L) \rangle$ (equation (3)). The slope gives $\gamma/\nu = 1.867 \pm 0.028$.

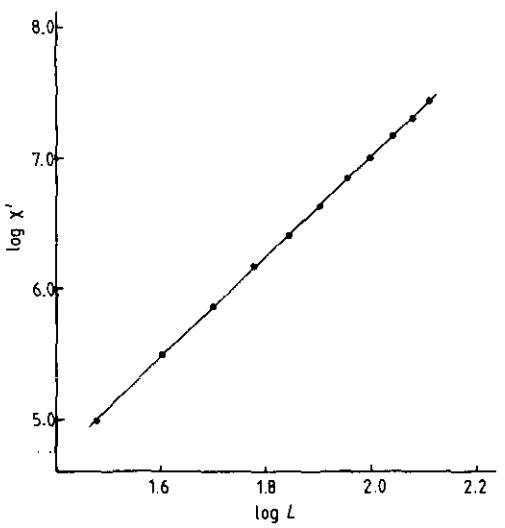

Figure 3. For the triangular lattice, a plot of log χ' against log L. χ' is the second moment of the cluster size distribution. The slope of the straight line gives $\gamma'/\nu = 3.829 \pm 0.062$.

et al 1980)

$$\Delta(L) = [\langle p_c^2(L)\rangle - \langle p_c(L)\rangle^2]^{1/2} \sim L^{-1/\nu} \tag{7}$$

where $\Delta(L)$ gives the spread in the estimates of the percolation threshold $p_c(L)$ as determined by the binary search method. The lattice size was varied from $L=50$ to $L=140$ in steps of 10. The plot $-\log \Delta(L)$ versus $\log L$ was found to be a straight line with the slope $1/\nu = 0.396$ and $\nu = 2.53$. This value of ν was used to obtain the values of the exponents γ and β from the directly measured values of γ/ν, β/ν. In this paper we have extended the data for $\Delta(L)$ to smaller lattice sizes up to $L=30$. With the extended data, one finds a distinct curvature in the plot of $\log \Delta(L)$ versus $\log L$. Thus, $\Delta(L)$ is no longer given by (7). It has not been possible to find the appropriate curve which fits the data reasonably well. For the triangular lattice also, the data points of the plot $\log \Delta(L)$ versus $\log L$ cannot be fitted by any known curve and so no approximate estimate of ν from finite-size scaling analysis can be made.

3. Monte Carlo simulation

In this case, simulation is carried out for one particular lattice size. For the square lattice, the lattice on which clusters have been generated, is of size 140×140; for the triangular lattice, the size is 130×130. The value of the percolation threshold p_c is determined by the binary search method. Ten thousand clusters are generated by the single cluster growth method. The growth of a cluster is stopped when there is no further site available for occupation or when the size of the clusters exceeds a maximum size S_{max}. For the square and triangular lattices, S_{max} has the values 4095 and 2047, respectively. The quantities χ, the average cluster size, χ', the second moment of the cluster-size distribution, as well as the correlation length ξ are determined as a function of $|p - p_c|$. As the site occupation probability p tends towards the percolation threshold, χ, χ' and ξ diverge as

$$\chi \sim |p - p_c|^{-\gamma} \tag{8a}$$

$$\chi' \sim |p - p_c|^{-\gamma'} \tag{8b}$$

$$\xi \sim |p - p_c|^{-\nu}. \tag{8c}$$

The correlation length ξ is determined from the relation (Stauffer 1985)

$$\xi^2 = \frac{2\,\Sigma_s' R_s^2 S P_s(p)}{\Sigma_s' S P_s(p)} \tag{9}$$

where $P_s(p)$ is the cluster size distribution defined in (2), R_s^2 is the square of the radius of gyration of a cluster of size S given by

$$R_s^2 = \sum_{i=1}^{s} \frac{|r_i - r_0|^2}{S} \qquad r_0 = \sum_{i=1}^{s} r_i/S \tag{10}$$

r_0 is the position of the centre of mass of the cluster and r_i the position of the ith site of the cluster. We first quote the results for the square lattice. The value of p_c is $p_c = 0.711 \pm 0.001$. Figure 4 shows a plot of $\log \chi$ versus $\log|p - p_c|$. The slope of the straight line obtained gives the value of the average cluster size exponent γ as $\gamma = 2.19 \pm 0.07$. The error on the average cluster size χ is determined from the cluster statistics, by calculating the variance σ of S in a sample of 10 000 clusters, the error

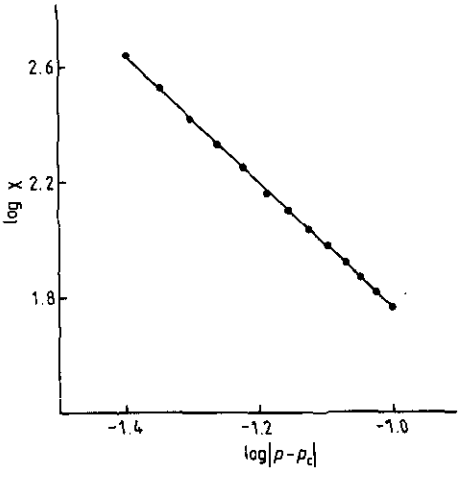

Figure 4. For the square lattice, a plot of $\log \chi$ against $\log|p-p_c|$. The slope gives $\gamma = 2.19 \pm 0.07$ (equation (8*a*)).

estimate of χ being $\sigma/100$. For this purpose, the clusters generated are counted in separate bins, the ith bin containing clusters of sizes in the range 2^{i-1}–(2^i-1). The asymptotic formula (8*a*) seems to work well for the range of values of $|p-p_c|$ between 0.04 and 0.10, and χ between 50 and 440. For values of $|p-p_c|$ less than 0.04, deviation from straight line behaviour occurs as the number of clusters of size $S > S_{max}$ (which have not been counted) begins to be appreciable. Figure 5 shows a plot of $\log \chi'$ versus $\log|p-p_c|$ (equation (8*b*)) from which the exponent γ' is obtained as $\gamma' = 4.51 \pm 0.16$. Figure 6 is a plot of $\log \xi$ versus $\log|p-p_c|$ (equation (8*c*)) from which the exponent ν is obtained as $\nu = 1.16 \pm 0.01$. From the scaling relation $\nu = (\gamma' - \gamma)/2$, the value of ν turns out to be $\nu = 1.16 \pm 0.23$, which agrees well with the value obtained through direct measurement. We now give the results for the triangular lattice. The value of p_c is $p_c = 0.667 \pm 0.001$. Figure 7 shows the plot of $\log \chi$ versus $\log|p-p_c|$, from which the

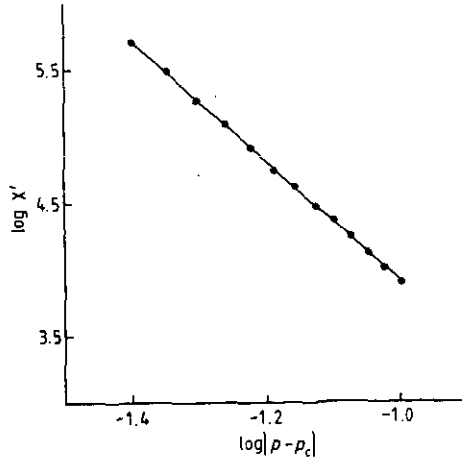

Figure 5. For the square lattice, a plot of $\log \chi'$ against $\log|p-p_c|$. The slope gives $\gamma' = 4.51 \pm 0.16$ (equation (8*b*)).

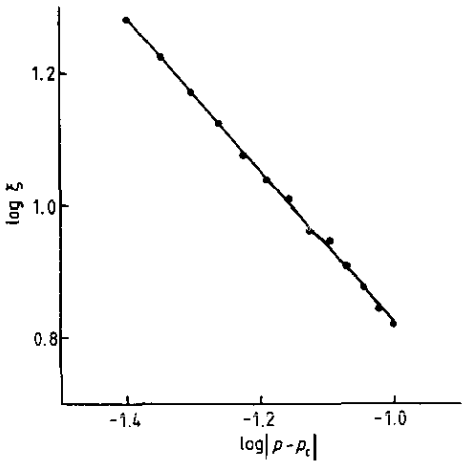

Figure 6. For the square lattice, a plot of $\log \xi$ against $\log|p-p_c|$. The slope gives $\nu = 1.16 \pm 0.01$ (equation (8*c*)).

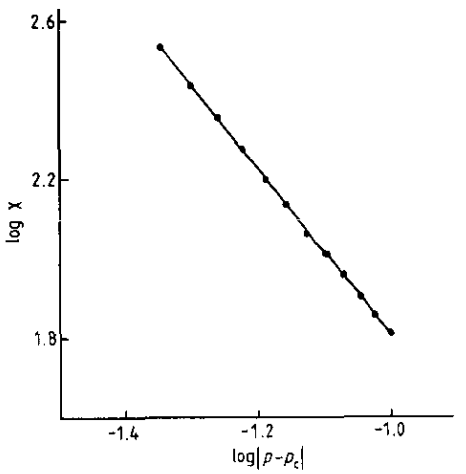

Figure 7. For the triangular lattice, a plot of $\log \chi$ against $\log|p-p_c|$. The slope gives $\gamma = 2.079 \pm 0.062$.

exponent $\gamma = 2.079 \pm 0.062$. Figure 8 is the plot of $\log \chi'$ versus $\log|p-p_c|$, from which the exponent $\gamma' = 4.376 \pm 0.199$. Figure 9 shows the plot of $\log \xi$ versus $\log|p-p_c|$, from which the value of ν is obtained as $\nu = 1.012 \pm 0.025$. The value of ν obtained from the scaling relation $\nu = (\gamma' - \gamma)/2$ is $\nu = 1.15 \pm 0.26$.

4. Series expansion method

The details of this method are given in standard reviews on percolation theory (Stauffer 1979, Essam 1980). We discuss the method only in relation to our problem. Briefly, the probability p that the origin from which clusters grow is occupied can be written

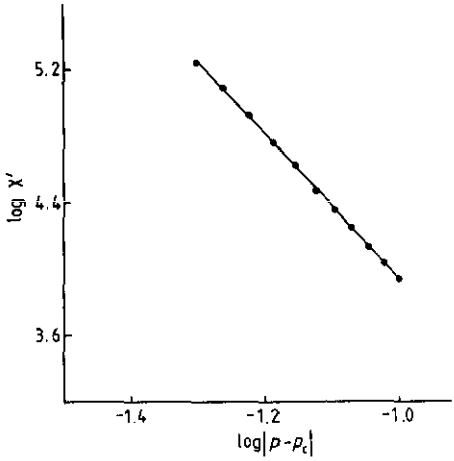

Figure 8. For the triangular lattice, a plot of $\log \chi'$ against $\log|p-p_c|$. The slope gives $\gamma' = 4.376 \pm 0.199$.

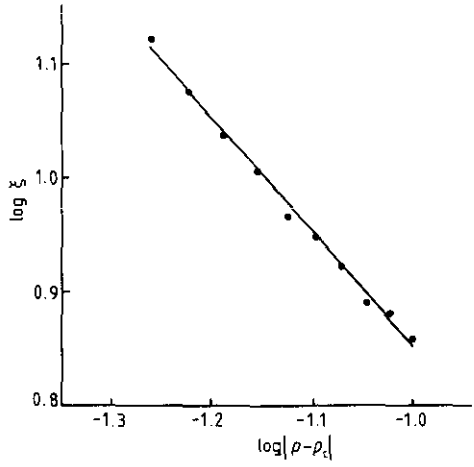

Figure 9. For the triangular lattice, a plot of $\log \xi$ against $\log|p-p_c|$. The slope gives $\nu = 1.012 \pm 0.025$.

as a sum over all finite clusters that start from it (for $p < p_c$), i.e.

$$p = \sum_{s,t} g_{st} p^s (1-p)^t = \sum_s p^s D_s(q) \qquad q = 1-p \tag{11}$$

where g_{st} is the number of clusters or 'lattice animals' of s sites and t perimeter sites and $D_s(q)$s are the perimeter polynomials. The animals are rooted at the origin. The average cluster size χ is the first moment of the cluster size distribution (Conceição *et al* 1986)

$$\chi = \sum_{s,t} s g_{st} p^s (1-p)^t \sim |p-p_c|^{-\gamma} \qquad \text{as } p \to p_c. \tag{12}$$

The clusters rooted at the origin obey the same rotational constraint as in the percolation process. Recently, lattice animals obeying the rotational constraint, designated as spiral lattice animals, have been studied extensively (Bose and Ray 1987, Bose *et al* 1988a, b,

Santra and Bose 1989). The major focus in these studies has been on spiral lattice site animals with no fixed origin. If the origin is not kept fixed, the number of perimeter sites is dependent on the position of the origin. In rotationally constrained percolation, the percolation clusters are rooted at the origin, so the spiral lattice site animals in the series expansion method have to be rooted, i.e. with a fixed origin, and each distinct animal configuration has a unique value for the number of perimeter sites. The rooted spiral lattice site animals of s sites and t perimeter sites have been enumerated exactly up to size $s = 13$ for clusters embedded in the square lattice. Thus, the series expansion for the average cluster size χ (equation (12)) is exactly known, when expanded in powers of p, up to the term containing the power p^{13}. A standard method (Sykes and Glen 1976) enables one to extend the series by one more power. Table 2 gives the coefficients for the expansion of $\chi = 1 + \Sigma_r b_r p^r$ on taking out a common factor of p. In the appendix we also list the perimeter polynomials for the spiral lattice site animals on the square lattice. After obtaining the series for χ, we have followed the procedure described in detail by Gaunt and Guttmann (1974). We form Padé approximants to the series for $\mathrm{d}/\mathrm{d}p(\ln \chi)$. In some cases the singularity closest to the origin lies on the negative real axis which is responsible for slow convergence of the approximants. Table 3 lists some sequences of D log Padé estimates of poles and residues. In figure 10, the residues are plotted against the positions of their corresponding poles. The

Table 2. Coefficients of the series of average cluster size $\chi = 1 + \Sigma_r b_r p^r$ for site percolation on the square lattice.

r	b_r
1	4
2	8
3	12
4	20
5	32
6	56
7	84
8	144
9	212
10	368
11	556
12	922
13	1328

Table 3. D log Padé estimates of poles (P) and residues (R) corresponding to average cluster size on the square lattice.

	$N-2/N$		$N-1/N$		N/N		$N+1/N$		$N+2/N$	
N	P	R	P	R	P	R	P	R	P	R
3							0.6694	1.5984	0.6764	1.6943
4					0.6771	1.7049	0.6707	1.6133		
5	0.6316	1.1353	0.6486	1.3073	0.5908	0.6306	0.6395	1.2259	0.7075	2.1276
6	0.6395	1.1202	0.6295	1.0835	0.5532	0.3421				
7	0.6384	1.1907								

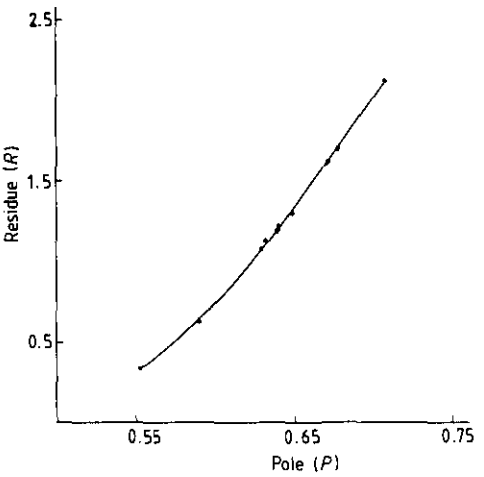

Figure 10. Pole residue plot corresponding to average cluster size for site percolation on the square lattice. The residue corresponding to the pole at $p_c = 0.711 \pm 0.001$ gives $\gamma = 2.167 \pm 0.004$.

data points define quite accurately a single smooth curve. The residue corresponding to the pole at p_c gives the exponent γ corresponding to the average cluster size χ. Since the value of p_c for spiral site percolation on the square lattice is not exactly known, we use the value $p_c = 0.711 \pm 0.001$ obtained from Monte Carlo simulation of spiral site percolation on the square lattice (section 3). The corresponding residue gives the exponent γ as $\gamma = 2.167 \pm 0.004$. For lack of a sufficiently long series, the series expansion method has not been applied to the triangular lattice.

5. Discussion

In sections 2, 3 and 4 we have used three different methods, finite-size scaling study, Monte Carlo simulation on a large lattice and series expansion, to calculate some critical exponents for spiral site percolation on the square and triangular lattices. Table 4 lists the values of the critical exponents obtained through different methods. For the sake of comparison of the finite-size scaling study and Monte Carlo simulation results, the values of γ/ν and γ'/ν in the case of Monte Carlo simulation have been computed from the directly measured values of γ, γ' and ν. For the triangular lattice, in computing γ/ν and γ'/ν the value of ν as obtained from scaling relation $\nu = (\gamma' - \gamma)/2$ has been used as it is closer to the estimate of ν for the square lattice. An examination of table 4 shows that universality of critical exponents holds within error bars.

The cluster size distribution function $P_s(p)$ has the scaling form in the critical region given by

$$P_s(p) = s^{-\tau+1} f[(p - p_c)s^{\sigma}] \tag{13}$$

where the exponents τ and σ are related to the exponents γ and β through the relations

$$\gamma = (3 - \tau)/\sigma \qquad \text{and} \qquad \beta = (\tau - 2)/\sigma. \tag{14}$$

A verification of the scaling function form in (13) is possible by plotting $P_s(p)/P_s(p_c)$ against $(p - p_c)s^{\sigma}$. If the scaling form is true then, for sufficiently large clusters and

Table 4. Numerical values of critical exponents for spiral site percolation on the square and triangular lattices.

Lattice type	Finite-size scaling			Monte Carlo Simulation			Series expansion
	γ/ν	γ'/ν	β/ν	γ	γ'	ν	γ
Square							
	2.01	4.05	0.043	2.19	4.51	1.16	2.167
	±0.06	±0.13	±0.009	±0.07	±0.16	±0.01	±0.004
				$\gamma/\nu = 1.89$	$\gamma'/\nu = 3.89$	$\nu = (\gamma' - \gamma)/2$	
				±0.08	±0.17	$= 1.16 \pm 0.23$	
					($\nu = 1.16$)		
Triangular							
	1.867	3.829	0.035	2.079	4.376	1.012	
	±0.028	±0.062	±0.008	±0.062	±0.199	±0.025	
				$\gamma/\nu = 1.808$	$\gamma'/\nu = 3.805$	$\nu = (\gamma' - \gamma)/2$	
					($\nu = 1.15$)	$= 1.15 \pm 0.26$	

for different values of p, the data should collapse onto a single curve. From (14), the exponents σ and τ can be expressed in terms of the exponents $1/\nu$, γ/ν and β/ν as

$$\sigma = \frac{1/\nu}{\gamma/\nu + \beta/\nu} \qquad \tau = \frac{3\beta/\nu + 2\gamma/\nu}{\gamma/\nu + \beta/\nu}. \tag{15}$$

On using the values of $1/\nu$, γ/ν (Monte Carlo simulation) and β/ν (finite-size scaling) the values of σ and τ for the square lattice are $\sigma = 0.446 \pm 0.024$ and $\tau = 2.022 \bullet 0.006$. The test of scaling form has been done for a lattice size of 140×140 with p_c equal to $\langle p_c(L) \rangle$. $P_s(p)$ and $P_s(p_c)$ have been calculated using (2) where N_s is the number of clusters in a particular bin, the size s being the geometric mean of the bounding cluster sizes of the bin. Figure 11 shows a plot of $P_s(p)/P_s(p_c)$ against the scaling variable

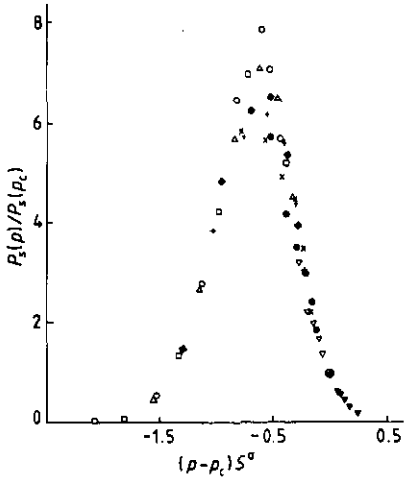

Figure 11. For the square lattice, a plot of $P_s(p)/P_s(p_c)$ against $(p - p_c)s^\sigma$ for nine different values of p with $\sigma = 0.446$. $|p - p_c|$ changes from 0.01 to 0.08 in steps of 0.01 with $32 < S < 2047$. The circled plus sign is the position of the point (0, 1). The data plotted correspond to: $p - p_c$ (inverted solid triangle), −0.01 (inverted open triangle), −0.02 (solid circle), −0.03 (cross), −0.04 (plus sign), −0.05 (solid diamond), −0.06 (open triangle), −0.07 (open square), −0.08 (open circle).

$(p-p_c)s^\sigma$ for nine different values of p. The data for different values of p have been marked by different symbols, $|p-p_c|$ being in the range 0.01–0.08. The cluster size s is within the limits $32<s<2047$. The circled plus denotes the location of the point (0, 1). In paper I, a test of the scaling form was done for $\sigma=0.19$. This value of σ was obtained from (15) with the overestimated value of $\nu=2.53$. The data collapse was not sharp and $|p-p_c|$ was in the range 0.01–0.055. On extending this range, we find that data collapse does not occur. With our new estimate of $\sigma=0.446$, data collapse occurs for the whole range of $|p-p_c|$, 0.01–0.08, for which data can be obtained. For $|p-p_c|>0.08$ the ratio $P_s(p)/P_s(p_c)$ becomes small. Figure 12 shows data collapse for the triangular lattice for which $\sigma=0.473$. The range for $|p-p_c|$ is 0.02–0.12 and the cluster size s is within the limits $64<s<511$.

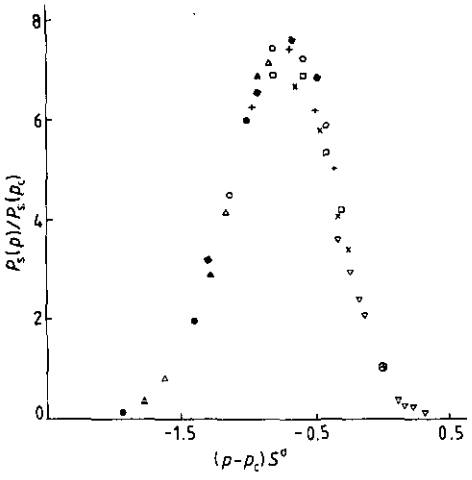

Figure 12. For the triangular lattice, a plot of $P_s(p)/P_s(p_c)$ against $(p-p_c)s^\sigma$ for 10 different values of p with $\sigma=0.473$. $|p-p_c|$ falls in the range 0.02–0.12 with $64<S<511$. The circled plus sign is the position of the point (0, 1). The data plotted correspond to $|p-p_c|=0.02$ (inverted open triangle), 0.04 (cross), 0.05 (open square), 0.06 (plus sign), 0.07 (open circle), 0.08 (solid diamond), 0.10 (open triangle), 0.11 (solid triangle), 0.12 (solid circle).

The values of the critical exponents obtained for spiral site percolation in two dimensions are different from the values of critical exponents in the case of undirected percolation. Spiral percolation is similar in nature to directed percolation, since for both the models a directional constraint is operative. In the first case the directional constraint is rotational in nature and in the second case percolation occurs only in certain specific directions. Dhar and Barma (1981) have studied directed percolation on the square lattice using Monte Carlo simulation. In table 5 we compare the values of the exponents obtained by them with the values of exponents obtained by us for spiral site percolation on the square lattice. We find that the average cluster size exponent γ is the same for both the cases. This is an interesting result which shows that the average cluster size diverges with the same exponent irrespective of the nature of the external constraint. One crucial difference between spiral and directed percolation is that in the first case percolation clusters grow isotropically whereas in the second case the clusters grown are anisotropic in nature. For the first case, there is thus only one correlation length which diverges with the exponent ν as $p\to p_c$ whereas, in the

Table 5. Comparison of the values of the critical exponents γ, β, τ and σ in the cases of directed and spiral percolation on the square lattice.

Percolation model	γ	β	τ	σ
Directed†	2.19 ± 0.03	0.240 ± 0.006	2.112 ± 0.005	0.406 ± 0.005
Spiral	2.19 ± 0.07	0.050 ± 0.005‡	2.022 ± 0.006	0.446 ± 0.024

† Monte Carlo simulation results (Dhar and Barma 1981).
‡ The value has been obtained by multiplying the value of β/ν for the square lattice (see table 3) by $\nu = 1.16$.

second case, there are two correlation lengths, one parallel and the other perpendicular to the preferred direction, which diverge with the exponents $\nu_{\parallel}$ and $\nu_{\perp}$ respectively as $p \to p_c$.

In our study of spiral site percolation on the square lattice, we have not been able to consider large lattice sizes. The major reason for this, in our case, is the non-availability of adequate computer time and memory. In this context we mention one significant limitation of the computer algorithm for the generation of rotationally constrained clusters. For simulation in the cases of both undirected and directed percolation, it is not necessary to store the whole lattice with all its L^d sites, where d is the dimension of the lattice. In two dimensions, knowledge of only one row (or column) is required at a time. For example, for a 1000×1000 lattice, only one array of size 1001 is necessary for storing the occupation status. This makes simulation of large systems possible. For spiral percolation (details of the algorithm given in paper I), however, the occupation status of the whole lattice has to be kept stored and so simulation of large systems becomes much more difficult. On the other hand, enumeration of spiral lattice site animals is time consuming because of the rotational constraint, thus limiting the scope of series expansion studies. Accurate estimates of the critical exponents are available in the cases of undirected and directed percolation. To achieve comparable accuracy, greater computational efforts are required in the case of spiral percolation.

Acknowledgments

The authors gratefully acknowledge helpful discussions with Deepak Dhar, Mustansir Barma and B K Chakrabarti. The authors thank the referees for useful suggestions and also for pointing out an important error in the original manuscript. The authors thank the Distributed Information Centre, Bose Institute, for providing computational facilities.

Appendix

Perimeter polynomials for the rooted spiral lattice site animals on the square lattice:

$D_1 = q^4$

$D_2 = 4q^5$

$D_3 = 4q^5 + 10q^6$

$$D_4 = 24q^6 + 20q^7$$

$$D_5 = 14q^6 + 84q^7 + 35q^8$$

$$D_6 = 4q^6 + 100q^7 + 232q^8 + 56q^9$$

$$D_7 = 4q^6 + 56q^7 + 448q^8 + 552q^9 + 84q^{10}$$

$$D_8 = 48q^7 + 404q^8 + 1548q^9 + 1200q^{10} + 120q^{11}$$

$$D_9 = 24q^7 + 361q^8 + 2020q^9 + 4600q^{10} + 2444q^{11} + 169q^{12}$$

$$D_{10} = 4q^7 + 268q^8 + 2132q^9 + 8144q^{10} + 12\,292q^{11} + 4776q^{12} + 244q^{13} + 4q^{14}$$

$$D_{11} = 122q^8 + 2016q^9 + 10\,348q^{10} + 28\,332q^{11} + 30\,476q^{12} + 9080q^{13} + 418q^{14} + 24q^{15} + 4q^{16}$$

$$D_{12} = 36q^8 + 1336q^9 + 11\,724q^{10} + 43\,572q^{11} + 88\,456q^{12} + 71\,456q^{13} + 17\,152q^{14} + 924q^{15} + 140q^{16} + 24q^{17} + 4q^{18}$$

$$D_{13} = 7q^8 + 692q^9 + 10\,222q^{10} + 57\,384q^{11} + 163\,802q^{12} + 254\,176q^{13} + 161\,084q^{14} + 32\,876q^{15} + 2671q^{16} + 616q^{17} + 148q^{18} + 24q^{19} + 4q^{20}.$$

References

Alexandrowitz Z 1980 *Phys. Lett.* **80A** 284

Bose I and Ray P 1987 *Phys. Rev.* B **35** 2071

Bose I, Ray P and Dhar D 1988a *J. Phys. A: Math. Gen.* **21** L219

Bose I, Ray P and Mukhopadhyay S 1988b *J. Phys. A: Math. Gen.* **21** L979

Conceição M da, Carvalho T P and Duarte J A M S 1986 *Z. Phys.* B **62** 239

Dhar D and Barma M 1981 *J. Phys. C: Solid State Phys.* **14** L1

Essam J W 1980 *Rep. Prog. Phys.* **43** 833

Gaunt D S and Guttmann A J 1974 *Phase Transitions and Critical Phenomena* vol 3, ed C Domb and M S Green (London: Academic) p 181

Leath P L 1976 *Phys. Rev.* B **14** 5046

Levinshtein M E, Schklovskii B I, Shur M S and Efros A L 1976 *Sov. Phys.-JETP* **42** 197

Reynolds P J, Stanley H E and Klein W 1980 *Phys. Rev.* B **21** 1223

Santra S B and Bose I 1989 *J. Phys. A: Math. Gen.* **22** 5043

—— *1991 J. Phys. A: Math. Gen.* **24** 2367

Stauffer D 1979 *Phys. Rep.* **54** 1

—— 1985 *Introduction to Percolation Theory* (London: Taylor and Francis)

Sykes M F and Glen M 1976 *J. Phys. A: Math. Gen.* **9** 87